





Indium Reduction Above 70% in SHJ Solar Cells: Study of the Module Stability

Adeline Lanterne¹, Remi Monna¹, Frédéric Jay¹, Tristan Gageot¹,
Raphael Cabal¹, Christine Denis¹ and Benjamin Thiriot¹

¹ Univ. Grenoble Alpes, CEA, Liten, Campus INES, 73375 Le Bourget du Lac, France

*Correspondence: Adeline Lanterne, adeline.lanterne@cea.fr

Abstract. This work focuses on reducing In-based TCO thicknesses to their minimum in SHJ solar cells with the goal to demonstrate the possibility of a drastic reduction of indium consumption in the fabrication process. On the front side, the reduction of the ITO thickness down to 15 nm implies to deposit an additional anti-reflective layer. Three anti-reflective dielectric layers have been studied (SiN_x , SiO_x and a bilayer $\text{SiN}_x/\text{SiO}_x$) in solar cell and module configurations to maximize the performances and evaluate the module stability under UV exposure. Lower J_{sc} losses after 120 kWh of UV exposure are measured with the use of thinner ITO layers, in agreement with a lower EQE deterioration in the IR range. The use of SiN_x dielectric results in the highest stability under UV and to the best performances after 120 kWh. Following further optimizations of the dielectrics and TCO, the 15 nm of ITO/ SiN_x option was combined with a thin IMO:H TCO on the rear side. TCO thicknesses down to 30 nm were studied on the rear side resulting in overall indium reduction of 77.2% with very limited efficiency loss at the cell level (below 0.1% absolute after light-soaking). Module reliability of these very low indium content solar cells was studied under UV and damp heat treatments highlighting lower degradations than reference cells for UV and promising results after damp heat test.

Keywords: Silicon Solar Cells, Heterojunction, Indium, Transparent Conductive Oxide, Reliability, UV, Damp Heat.

1. Introduction

While heterojunction solar cells (SHJ) demonstrate the highest performances for single junction solar cells based on crystalline silicon with efficiency reaching 27.09% [1], SHJ technology is an attractive candidate for new industrial productions due to several other advantages. Among them we can note the low temperature ($<230^\circ\text{C}$) and low number of process steps required [2], the low temperature coefficient ($<-0.27\%/\text{C}$), the compatibility with thin wafers below 100 μm and the strong adaptability to the tandem technology. In SHJ cells, the carrier selective layers are based on intrinsic and doped hydrogenated amorphous silicon layer (a-Si:H), contacted by a transparent conductive oxide (TCO) layer and metal electrodes. This TCO layer must fulfill several requirements in order to maximize the cell efficiency. It includes a low contact resistance with the active layers and the metal grids, a low sheet resistance to provide a high lateral transport toward the electrode, but also a high transmittance and it must play the role of an efficient antireflective layer. All these requirements are provided by indium based materials, leading to the current use of indium tin oxide (ITO) as mainstream TCO.

However indium increases the dependency of SHJ solar cells on scarce raw materials due to its limited production and its use in other competitive high value-added technologies [3].

The use of indium limits today the potential increase of the SHJ annual production capacity below 100 GW/year for a consumption of 20% of the 2019 global indium supply as calculated in [4]. In consequence, to allow a strong increase of the volume production, the usage of indium must be reduced or removed from SHJ solar cells [5] and active researches are conducted in that way. One option, shown in Figure 1, is to reduce the indium-based TCO layer thickness while adding a dielectric ($\text{SiN}_x\text{:H}$, $\text{SiO}_x\text{:H}$, ...) as a double antireflective coating (DARC) layer [6], [7]. Another way is based on the development of indium-free TCO such as AZO or SnO_2 [8], [9], [10], or the use of multilayers of In-free and In-based TCO [11], [12] as In-free TCO are facing stability issues under humidity [13], [14].

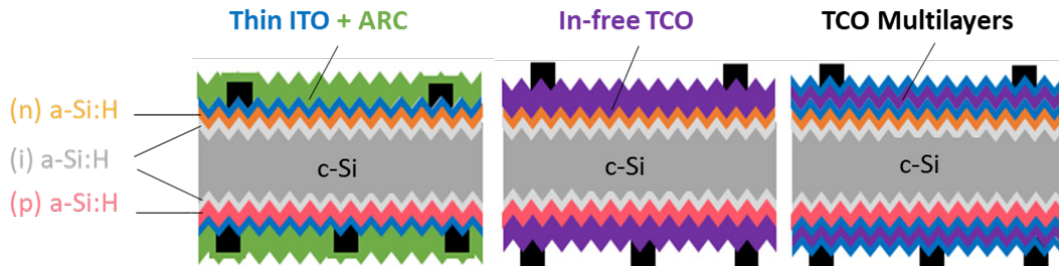


Figure 1. SHJ solar cells schemes with three Indium reduction approaches.

In this context, this work has been focused on keeping indium based TCO layers while reducing their thicknesses to the lowest on the front and rear side of the cell with the aim to investigate the module reliability of this approach. On the front side (FS), we used a highly conductive thin ITO layer of 15 nm [15] and studied the impact of the dielectric layer on the module degradation under UV. The FS 15 nm of ITO was then combined with a hydrogenated indium metal oxide (IMO:H) on the rear side (RS) [16], with thickness reduced down to 30 nm before performing aging tests in module configuration.

2. Experimental

In this work, standard rear emitter 6 busbars SHJ solar cells were processed on M2 n-type Cz wafers with a-Si:H based carrier selective layers. For "reference" solar cells, 100 nm of ITO is deposited on the front side and 100 nm of IMO:H on the rear by PVD before screen-printing of the metallic grid with a silver paste. Here and in all this paper the TCO thicknesses correspond to equivalent thicknesses measured on flat surface by ellipsometry. To study the front dielectric, the reference cells were compared to a front thin ITO of 15 nm with an anti-reflective dielectric deposited by PECVD after the metallization step, forming a double antireflective coating (DARC). This front side structure was later combined with a highly conductive 40 nm or 30 nm of IMO:H layer on the rear side. For this integration, a selective layer based on hydrogenated nanocrystalline silicon ((n) nc-Si:H) was also investigated on the front to relax the conductivity required for the TCO. The metallization grid was identical on all cells in this paper.

Solar cells were interconnected in one $\frac{1}{2}$ cell or two $\frac{1}{2}$ cells strings, followed by lamination in glass-glass (GG) or glass-backsheet (GBS) configuration. A TPO low cut off encapsulant was used for UV aging treatments, that were performed in irradiance of 200 W/m^2 at 80°C and a POE encapsulant was used for damp heat (DH) tests, performed in a chamber at 85°C with 85% relative humidity. All the tests followed the standards IEC 61215 – MQT16 [17].

3. Results and Discussion

3.1 Study of the front dielectric

Three dielectrics options were studied as DARC layers on the top of the FS 15 nm ITO: SiN_x, SiO_x, and a bilayer SiN_x/SiO_x. In this study the dielectric thicknesses were optimized to maximize the solar cell efficiency in air, without taking into account the impact of the module encapsulant. After optimization, SHJ solar cells were fabricated with the three DARC approaches and compared to reference SHJ with a front 100 nm of ITO. The cells with the SiO_x DARC and the bilayer DARC featured an improved current as compared to the reference cells (J_{sc} increase of 0.2 mA/cm²) resulting in a higher median efficiency values of 22.6% and 22.7% respectively as compared to 22.5% of efficiency for the reference cells and 22.4% for the SiN_x DARC cells.

Four one ½ cell mono-modules in GG configuration were laminated for each cell batch: Reference, DARC SiO_x, DARC SiN_x/SiO_x and DARC SiN_x. After lamination the modules with DARC SiN_x/SiO_x show a maximal power (P_{max}) similar to the reference (see Figure 2) while modules with DARC SiO_x exhibit a slightly lower P_{max} than others due to a lower J_{sc} value. Figure 3 presents the EQE measurements before and after UV exposure. Before UV, an improved EQE response in the short wavelength range was observed for all the thin ITO modules with DARC layer. This improvement was attributed to a reduced parasitic light absorption in thin ITO layer of 15 nm as compared to the ITO of 100 nm in the reference cells.

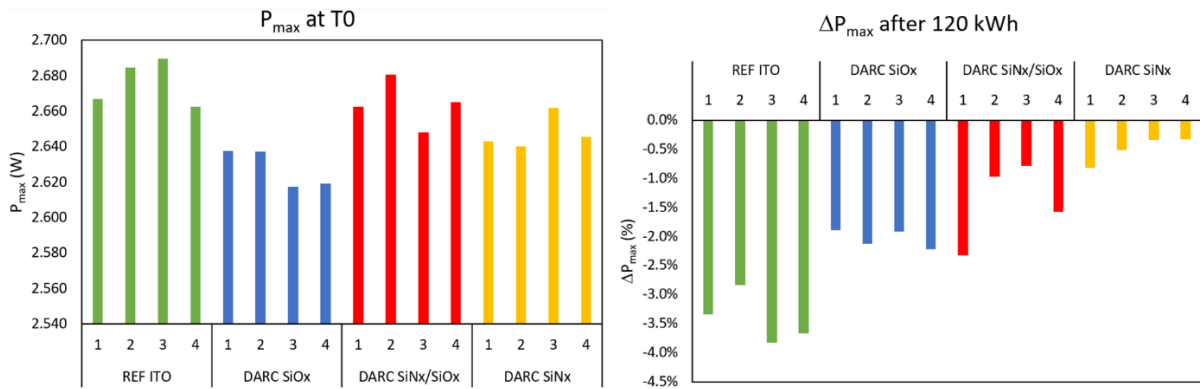


Figure 2. (left) Maximal power measured on the four individual modules fabricated per batch before UV exposure and (right) its relative variation after 120 kWh of UV exposure.

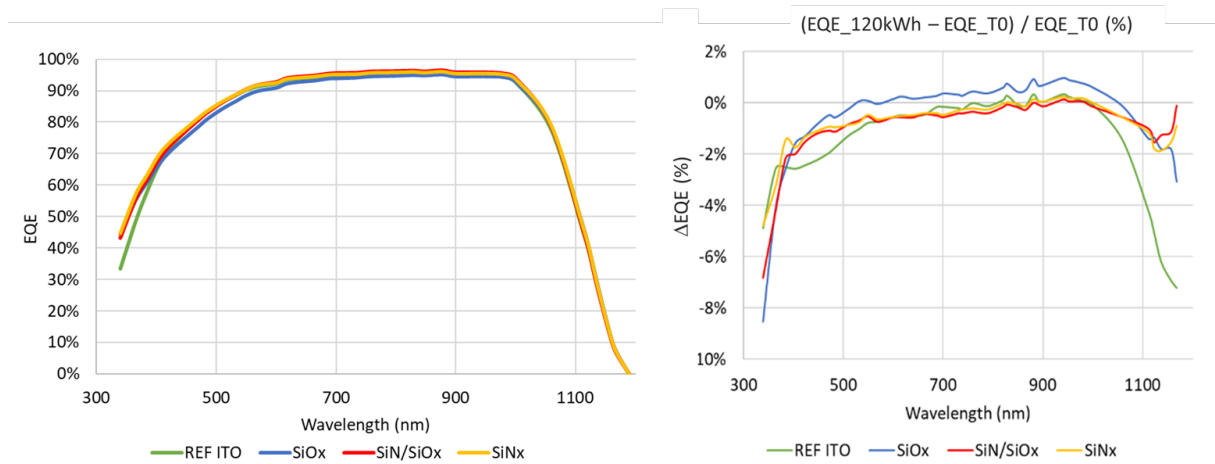


Figure 3. (left) EQE curves of the modules before UV exposure and (right) their relative variations after 120kWh of UV exposure. Each curve corresponds to the average curve of the four individual modules measured per batch.

After 120 kWh of UV, a lower degradation of P_{max} was measured for all modules with a thin ITO and DARC layer as compared to the reference modules (cf. Figure 2). The deterioration of the reference modules under UV is explained by higher J_{sc} losses, which can be correlated to an important decrease of the EQE in the IR range (green curve of Figure 3). This EQE behavior of reference SHJ modules was previously observed in our work [15], one possible explanation is an increase of the free carrier absorption in the ITO due to hydrogen migration and doping of the TCO [18]. In conclusion, the SiN_x capping modules demonstrate the best stability under UV in agreement with lower EQE losses in the short wavelength range than other DARC modules. After 120 kWh of UV, SiN_x modules feature the highest average P_{max} , exceeding the reference.

3.2 Combination of front and rear Indium reduction

3.2.1 Solar cells performances

Following previous results, the front stack of 15 nm of ITO with SiN_x DARC was further optimize. Particularly, the SiN_x thickness was modified to maximize the module efficiency. This front structure was then combined with a reduced TCO thicknesses on the rear side. In that goal, rear IMO:H layers of 40 nm and 30 nm were developed and integrated in SHJ with a front 15 nm of ITO, resulting in an overall indium reduction of 72.1% and 77.2% respectively as compared to solar cells with 200 nm of ITO (FS + RS). Reference cells (ITO 100 nm + IMO:H 100 nm) and low indium content solar cells (ITO 15 nm + IMO:H 40 nm or 30 nm) were fabricated either with a front (n) a-Si:H selective layer, or with a (n) nc-Si:H layer. The solar cells I(V) parameters were then measured before and after a light soaking (LS) treatment (performed on a limited number of cell, cf. Figure 4).

Results before LS are shown in Table 1, they highlight a decrease of the FF and V_{oc} with the reduction of the TCO thicknesses along with an opposite improvement of the J_{sc} . The FF decrease is related to a small sheet resistance increase for the 15 nm thin ITO layer as compared to the 100 nm ITO layer, which induces a reduction of the lateral transport. The V_{oc} deterioration can be explained by an increase of the remaining sputtering damages with thinner TCO deposition that were not sufficiently annealed as observed in [19]. Finally the higher J_{sc} is linked to better transparency and the light management in the FS DARC along with a back reflector effect from thinner TCO at the rear side.

We can also notice that due to higher conductivity and better contact with the FS thin TCO, the use of a (n) nc-Si:H as active layer leads to limit FF loss and improved cells efficiency. The median efficiency loss measured for an indium reduction of 77.2%, is then reduced down to 0.16% absolute, against 0.4% absolute with a (n) a-Si:H active layer.

Table 1. I(V) parameters measured on each solar cells batch (median values of 20 to 50 cells). All cells with 15 nm of ITO have a SiN_x DARC layer.

(n) selective layer	ITO (nm)	IMO:H (nm)	In reduction from 200 nm of ITO	V_{oc} (mV)	J_{sc} (mA/cm ²)	FF (%)	Eff. (%)	Batches used for Module
a-Si:H	100	100	+1%	737.3	38.08	80.0	22.44	x
a-Si:H	15	40	-72.1%	736.2	38.19	79.0	22.19	x
a-Si:H	15	30	-77.2%	735.2	38.27	78.3	22.04	
nc-Si:H	100	100	+1%	737.4	38.22	80.1	22.52	
nc-Si:H	15	40	-72.1%	736.7	38.23	79.6	22.38	x
nc-Si:H	15	30	-77.2%	736.5	38.26	79.5	22.36	x

After light soaking, similar FF and V_{oc} improvements are observed for reference cells and low indium content cells (cf. Figure 4), showing no specific impact of the indium reduction on the light-soaking effect. The main factors explaining the FF and V_{oc} gains are described in

[20], among them an improvement of the TCO conductivity was previously observed under light-soaking along with a decrease of the contact resistivity [20].

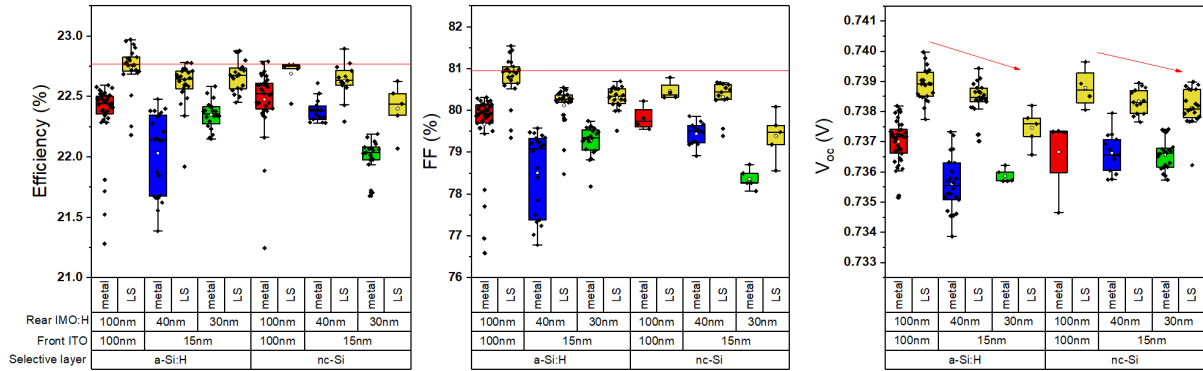


Figure 4. Efficiency, FF and V_{oc} before (metal) and after light soaking treatment (LS), performed on a limited number of cell of each batch of Table 1. All cells with 15 nm of ITO have a SiN_x DARC layer.

After LS, an even lower median efficiency loss of only 0.08% was measured for indium reduction of 77.2% with the nc-Si:H selective layer.

3.2.2 Module Reliability

After light soaking, solar cells of four batches were integrated in mini-module to investigate their reliability. The four batches are identified on Table 1 and modules integrating the SHJ solar cells of the first batch, with TCO of 100 nm on the front and rear sides, will be noted "REF a-Si" or "Reference".

To study their degradation under UV, three $\frac{1}{2}$ cell mono-modules in GBS configuration were laminated with a TPO low cut-off encapsulant. After 30 kWh, modules with thin TCO layers show lower J_{sc} decrease than the reference and a better EQE stability (see Figure 5 right). The reduction of the rear TCO did not impact the UV stability of the cells with a front 15 nm of ITO and SiN_x capping. The results confirm the advantages of using a thin ITO with SiN_x for UV stability, as highlighted in the previous study.

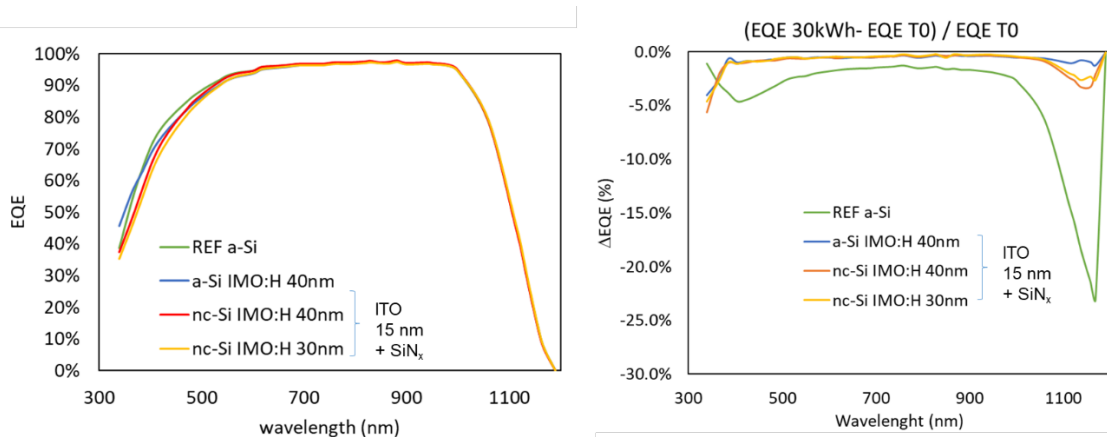


Figure 5. (left) EQE curves of the modules before UV exposure and (right) their relative variations after 30kWh of UV exposure. Each curve corresponds to the average curve of the three individual modules measured per batch.

The reliability under DH was then evaluated with mini-module of two $\frac{1}{2}$ cells in glass-glass configuration using a POE encapsulant. Three modules were laminated for each solar cells batch. Their initial performances, shown in Table 2, are not directly correlated to the solar cell performances due to the use of non-representative cells of each batch. We can notice that

the high FF obtained with the low indium content configurations, demonstrates the absence of interconnection issue with the deposition of a dielectric above the metallization.

Table 2. Average $I(V)$ parameters of mini-modules before DH treatment.

(n) selective layer	ITO (nm)	IMO:H (nm)	In reduction from 200 nm of ITO	I_{sc} (A)	V_{oc} (V)	FF (%)	P_{max} (W)
a-Si:H	100	100	+1%	4.600	5.921	77.7	21.17
a-Si:H	15	40	-72.1%	4.599	5.919	78.0	21.24
nc-Si:H	15	40	-72.1%	4.566	5.919	79.0	21.34
nc-Si:H	15	30	-77.2%	4.597	5.919	78.5	21.36

The module performances were evaluated after damp heat aging test. FF and V_{oc} variations are presented in Figure 6 and no variation of the V_{oc} was measured after DH. Up to 1000h of DH, modules with thin TCO thicknesses first exhibit a similar FF deterioration than reference SHJ. After 2000h and 3000h of DH, additional deteriorations of the FF for low-indium content modules are observed. However the limited extend of these drops results in promising ΔP_{max} variation of only 1.8% to 2.3% for the three low-indium batches after 2000h, thanks to very limited J_{sc} losses under DH. After 3000h of DH, modules with nc-Si:H layers succeed to pass three times the standard with P_{max} losses below 5% [17].

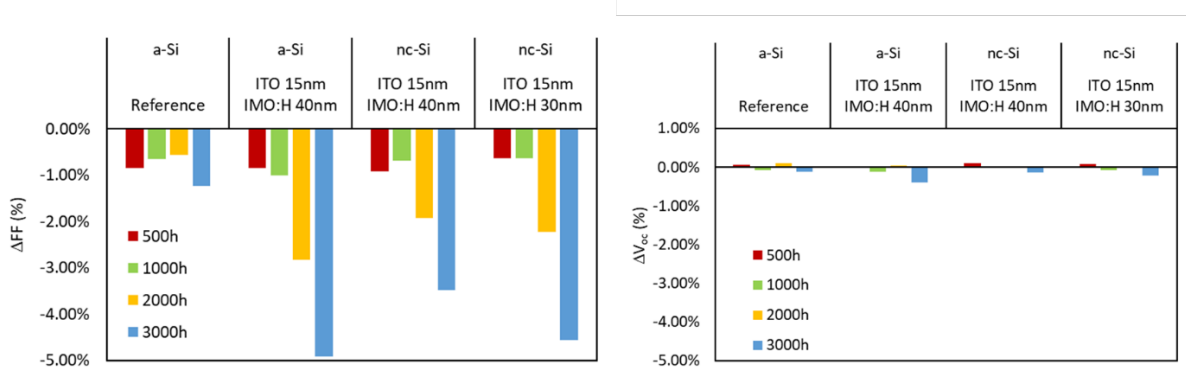


Figure 6. FF and V_{oc} relative variation after DH exposure. Average values of three mini-module.

4. Conclusion

In conclusion the possibility to reduce indium content in SHJ solar cells by 77.2% while reducing the cell efficiency of less than 0.1% absolute was demonstrated. Ultra-thin ITO of 15 nm was used on the front side for this demonstration with an additional DARC SiN_x layer combined with a reduced optimized IMO:H layer of only 30 nm on the rear. Module reliability of these cells were investigated. On the front side DARC SiN_x layer show better stability under UV than alternative SiO_x or SiN_x/SiO_x layers. But all SHJ modules with solar cells integrating 15 nm of ITO layer with DARC dielectrics exhibit an improved stability under UV as compared to reference modules with thick ITO, thanks to a lower EQE degradation especially in the IR range. Finally, modules with ultra-low indium-content SHJ solar cells show promising results under DH test with losses limited below 2.3% after 2000h using a glass-glass module configuration and only 30 nm of IMO:H on the rear side of the cells without any dielectric layers.

Data availability statement

Data will be made available on request.

Author contributions

The authors confirm contributions to the paper as follows: Supervision: A. Lanterne; Conceptualization: R. Monna, F. Jay and R. Cabal; Methodology: R. Monna, F. Jay and T. Gageot; Validation: A. Lanterne, R. Monna and F. Jay; Investigation: A. Lanterne, T. Gageot, R. Cabal, C. Denis, B. Thiriot; Visualization: A. Lanterne, F. Jay, T. Gageot; Writing and original draft: A. Lanterne.

Competing interests

The authors declare that they have no known competing financial interests or personal relationships that could have appeared to influence the work reported in this paper.

Funding & Acknowledgement

This work was supported by the RESILEX project that has received funding from the European Union under grant agreement No 101058583. The authors would like to acknowledge ENEL Green Power (EGP) for funding and for the extensive joint R&D development on the SHJ technology at CEA. Finally, the authors would like to acknowledge all the staff members from CEAINES who contributed for cells and modules manufacturing as well as for the reliability tests.

References

- [1] LONGI Sets a New World Record of 27.09% for the Efficiency of Silicon Heterojunction Back-Contact (HBC) Solar Cells – LONGI - Available online: <https://www.longi.com/en/news/heterojunction-back-contact-battery/> (accessed on 19 January 2024).
- [2] H. Lin, et al., *Nat. Energy*, vol. 8 (2023) 789–799. <https://doi.org/10.1038/s41560-023-01255-2>
- [3] M. Grohol, V. Constanz, et al., European Commission, «Study on the Critical Raw Materials for the EU 2023» 2023, <https://www.doi.org/10.2873/725585>.
- [4] Y. Zhang et al., *Energy Environ. Sci*, vol. 14 (11) (2021) 5587–5610. <https://doi.org/10.1039/D1EE01814K>
- [5] S.K. Chunduri, M. Schmela, et al., « Heterojunction Solar Technology 2023 Edition », *TaiyangNews*, 2023, <http://doi.org/10.13140/RG.2.2.22609.71522>.
- [6] C. Han et al., *Prog Photovolt Res Appl.*, Vol. 30 (2022) 750–762. doi:10.1002/pip.3550.
- [7] A. Cruz et al., *Sol. Energy Mater. & Sol. Cells*, vol. 236 (2022) 111493. doi:10.1016/j.solmat.2021.111493.
- [8] L.-L. Senaud et al., *IEEE J. Photovolt.*, vol. 12 (2022) 906–914. doi:10.1109/JPHOTOV.2022.3176983.
- [9] A. Cruz et al., *IEEE J. Photovolt.* , vol. 10 (2020) 703–709. doi:10.1109/JPHOTOV.2019.2957665.
- [10] T. Koida et al., *Sol. RRL*, Vol. 7 (2023) 2300381. doi:10.1002/solr.202300381.
- [11] P. Schmid et al., *IEEE J. Photovolt.*, vol. 13 (2023) 646–655. doi:10.1109/JPHOTOV.2023.3267175.
- [12] G. Dong et al., *Prog. Photovolt. Res. Appl.*, 31 (2023) 931-938. doi:10.1002/pip.3697.
- [13] T. P. Dhakal et al., *IEEE Transactions on Device and Materials Reliability*, vol. 12, no. 2, pp. 347-356, June 2012, doi:10.1109/TDMR.2012.2186574.A.B.
- [14] Morales-Vilches et al., *IEEE J. Photovoltaics*, vol. 9 (2019) 34–39. <https://doi.org/10.1109/JPHOTOV.2018.2873307>.
- [15] T. Gageot, et al., *Sol. Energy Mater. & Sol. Cells*, vol. 261, 2023, 112512. <https://doi.org/10.1016/j.solmat.2023.112512>.
- [16] F. Jay et al., *Sol. RRL*, vol. 7 (2022), 2200598. <https://doi.org/10.1002/solr.202200598>

- [17] EN IEC 61215-1:2021: Terrestrial photovoltaic (PV) modules - Design qualification and type approval - Part 1: test requirements'. (2021) Available: <https://www.boutique.afnor.org/fr-fr/norme/nf-en-iec-612151/modules-photovoltaiques-pv-pour-applications-terrestres-qualification-de-la/fa195378/238021>.
- [18] S. Kim et al., *Vacuum*, vol. 108, (2014) 39-44. <https://doi.org/10.1016/j.vacuum.2014.05.015>.
- [19] B. Demaurex et al., *Appl. Phys. Lett.*, vol. 101 (2012) 171604. <https://doi.org/10.1063/1.4764529>.
- [20] J. Veirman, et al., *AIP Conf. Proc.*, vol. 2487, (2022) 020017. <https://doi.org/10.1063/5.0089284>.